ACS SyntheticBiology

Research Article

pubs.acs.org/synthbio

Genetically Programmable Pathogen Sense and Destroy

Saurabh Gupta, Eran E. Bram, and Ron Weiss*

Department of Biological Engineering, Massachusetts Institute of Technology, Cambridge, Massachusetts 02139, United States

Supporting Information

ABSTRACT: *Pseudomonas aeruginosa* (*P. aeruginosa*) is a major cause of urinary tract and nosocomial infections. Here, we propose and demonstrate proof-of-principle for a potential cell therapy approach against *P. aeruginosa*. Using principles of synthetic biology, we genetically modified *E. coli* to specifically detect wild type *P. aeruginosa* (PAO1) via its quorum sensing (QS) molecule, $3OC_{12}HSL$. Engineered *E. coli* sentinels respond to the presence of $3OC_{12}HSL$ by secreting CoPy, a novel pathogen-specific engineered chimeric bacteriocin, into the extracellular medium using the flagellar secretion tag FlgM. Extracellular FlgM-CoPy is designed to kill PAO1 specifically. CoPy was constructed by replacing the receptor and translocase domain of Colicin E3 with that of Pyocin S3. We show that CoPy toxicity is PAO1 specific, not affecting sentinel *E. coli* or the other bacterial strains tested. In order to define the system's basic requirements and PAO1-killing capabilities, we further determined the growth rates of PAO1 under different conditions and concentrations of purified and secreted FlgM-CoPy. The integrated system was tested by co-culturing PAO1 cells, on semisolid agar plates, together with engineered sentinel *E. coli*, capable of secreting FlgM-CoPy when induced by $3OC_{12}HSL$. Optical microscopy results show that the engineered *E. coli* sentinels successfully inhibit PAO1 growth.

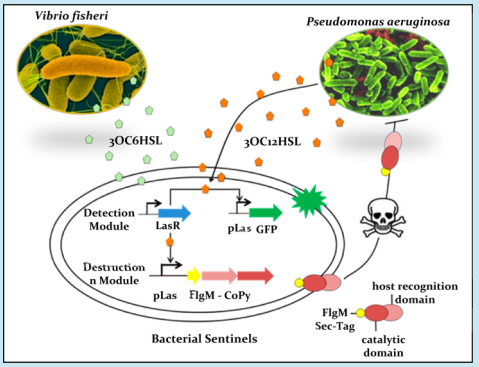

KEYWORDS: *chimeric proteins, bacteria, bacteriocin, colcin, pyocin, FlgM*

Synthetic biology uses engineering principles to design and create sophisticated systems that tackle medical and environmental problems. One such problem is the increase in multi-drug resistance among pathogenic bacteria. A significant cause for this problem is the widespread use of broad-spectrum antibiotics.[1] On the one hand, broad-spectrum antibiotics portend to have a high likelihood of being effective against unidentified pathogens, but unfortunately they also inhibit growth of non-pathogenic members of the human microbiome. Normal gut flora compete with pathogenic bacteria, and an individual becomes more susceptible to subsequent infections in the absence of helpful bacteria,[2] which often produces severe gastrointestinal disorders.[3] A potential solution to this problem is an autonomous antibacterial therapy that remains inert until a pathogen is detected and releases antibacterial compounds on-demand to kill the pathogen specifically. In this paper we engineer sentinel *E. coli* cells to specifically detect the QS molecule $3OC_{12}HSL$, produced by *P. aeruginosa*, and then synthesize and secrete a *P. aeruginosa* specific chimeric bacteriocin CoPy. This bacteriocin is secreted from the engineered *E. coli* cells with the aid of a flagellar secretion tag FlgM.

Bacteriocins are a type of naturally existing protein toxins, normally produced by bacteria under stressful conditions, which lead to the rapid elimination of neighboring cells that are not immune to their effect. Bacteriocins are highly toxic to closely related bacterial strains but not to their producing strain.[4,5] Bacteriocins are generally classified into two groups, termed A and B, based on cross-resistance pattern, cell entry mechanism (Tol/TonB receptors, respectively), and mechanism of release from producing cells (secreted/lysed out in SOS response, respectively).[6] Colicins are bacteriocins produced by certain strains of *E. coli* and are lethal to related *E. coli* strains. Accordingly, pyocins are analogous bacteriocins produced by certain strains of *P. aeruginosa*. The producing strains are unaffected since they co-produce an immunity protein against the bacteriocin. In known bacteriocin operons, the first gene encodes the activity protein, *cxa*, which stands for bacteriocin X activity. The gene encoding the immunity protein is designated either *cxi*, for bacteriocin X immunity, or *imX*, and is located downstream of the bacteriocin activity gene. Bacteriocin activity proteins have three distinct domains arranged from N to C terminus that include receptor, translocase, and nuclease (with immunity protein-binding) domains. The translocation domain and receptor binding domain are species specific. The nuclease domain is usually a DNase or RNase and kills the cell by cleaving its DNA or RNA.[4,5]

In this study, for PAO1 specific killing, we replaced the receptor and translocase domain of the group B colicin E3 with that of pyocin S3 to produce a chimeric bacteriocin termed CoPy that only targets PAO1.[7] The receptor domain of extracellular CoPy binds the corresponding receptor FpyA on the surface of *P. aeruginosa*, and the translocase domain of CoPy forms a complex with Ton transporters. Upon binding

Received: April 12, 2013
Published: June 13, 2013

   dx.doi.org/10.1021/sb4000417 | *ACS Synth. Biol.* 2013, 2, 715–723

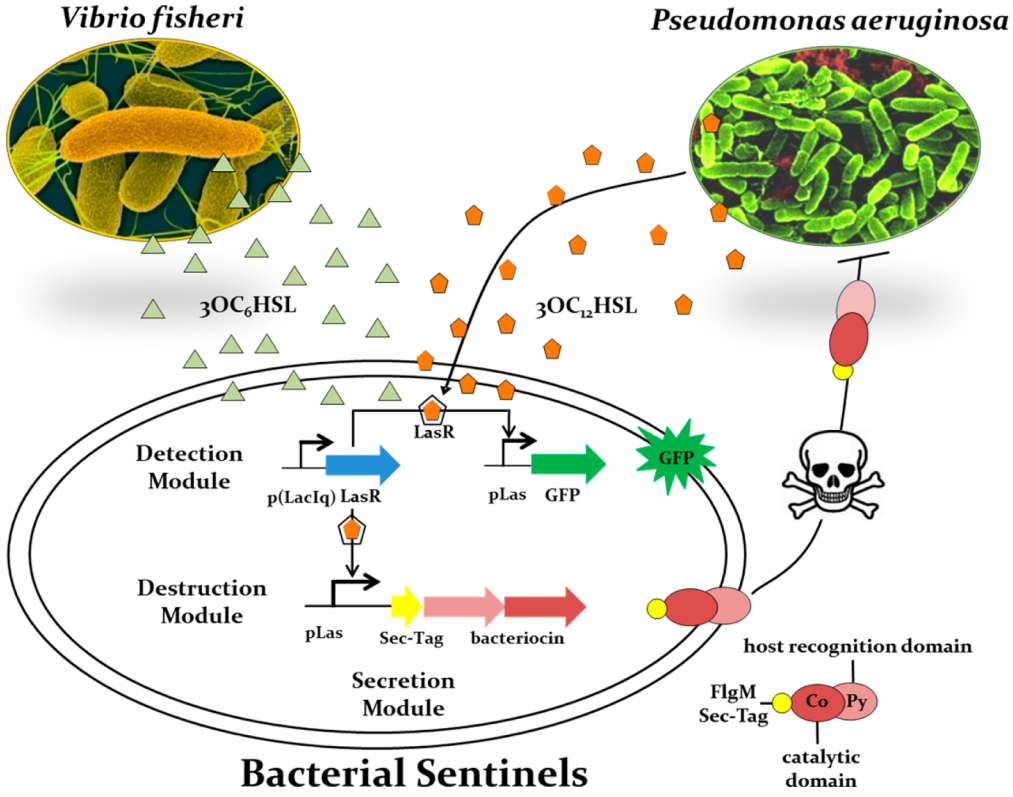

Figure 1. Architectural details of our Pathogen Sense and Destroy system. This system is divided into three modules. The first module is the Detection module where diffusible AHL autoinducer (produced by Gram-negative cells with an I/R system, e.g., *V. fischeri* or *P. aeruginosa*) is detected with an R-protein activated pathway in the sentinels. Detection of a specific AHL results in the production of a color-coded output. The second module is the Destruction module. When a pathogen is detected, this module will synthesize a pathogen-specific toxin, CoPy. The third module is the Secretion module that uses a secretion tag, FlgM, to transport the toxin into the environment and kill the pathogen specifically.

the cell surface receptor, the immunity protein breaks free and the nuclease domain enters the cell. *Pseudomonas* does not possess immunity against this nuclease domain as it originated from *E. coli*, hence leading to PAO1 death.

Efficient extracellular secretion of folded proteins without cell lysis presents a major hurdle for many biotechnology applications. Effective extracellular secretion requires a single-step secretion of intact, fully folded proteins in order to reduce accumulation in the periplasm. Gram-negative bacteria have seven known distinct secretion pathways, classified as Type I–VII, that enable transfer of proteins across the inner and outer membranes.[8−15] The complex Type IV system is only superficially characterized in *E. coli* and has not been employed for secretion or display of recombinant proteins thus far.[14] Type VI[16,17] and Type VII[18] (only identified in *Mycobacterium* spp.) secretion systems have only been recently identified, and the details about the secretion mechanism are still emerging. Type II and V are two-step secretion mechanisms. Type I, Sec, ABC, and Type III secretion systems secrete unfolded proteins.[19] Type III and IV secretion systems are mostly used by pathogenic bacteria to transport proteins from the bacterial cytoplasm to eukaryotic cytoplasm. The bacterial flagellar system is similar to the Type III system except that bacteria use it as a one-step mechanism to secrete partially folded flagellar components into the extracellular environment and to assemble flagella. The bacterial flagellum has been studied extensively in *Salmonella enterica serovar Typhimurium* and comprises an engine and a propeller that are joined by a flexible hook.[20−22] Upon completion of the flagellar hook-basal body (HBB) complex, FlgM is secreted from the cell, presumably through a completed HBB structure, and σ28-dependent transcription of late stage genes ensues. *E. coli* has similar flagellar control.

Below, we demonstrate that our synthetic cellular system is capable of detecting and specifically inhibiting the growth of wild type *P. aeruginosa* strain PAO1. In our efforts, we first characterized individual components and then connected them to create the complete Sense and Destroy system. We also calculate the number of engineered sentinels needed to kill an individual PAO1 cell in different system contexts.

RESULTS AND DISCUSSION

The architecture of our bacterial Sense and Destroy system against PAO1 (Figure 1) is divided into three interconnected modules. The first module is the 'Detection' module that enables bacterial sentinels to specifically detect PAO1 QS signaling molecules. The second 'Destruction' module produces PAO1 specific toxin, CoPy, as a result of sensing by the first module. The third 'Secretion' module enables sentinels to secrete CoPy with a secretion tag, FlgM. In the following sections we first present the results for characterizing the individual modules and then show experiments and analysis of co-culturing PAO1 with sentinels, harboring the full system, on semisolid agar plates.

Specific Detection and Destruction of PAO1. The sentinels were tested for their response to exogenous and endogenous $3OC_{12}HSL$ produced by PAO1 (Methods). Figure 2a shows that 10 μM of $3OC_{12}HSL$ is sufficient to elicit maximal response from the sentinels. To obtain a similar response, approximately 10^9 colony forming units (CFU) of PAO1 are needed (Figure 2b).

dx.doi.org/10.1021/sb4000417 | *ACS Synth. Biol.* 2013, 2, 715−723

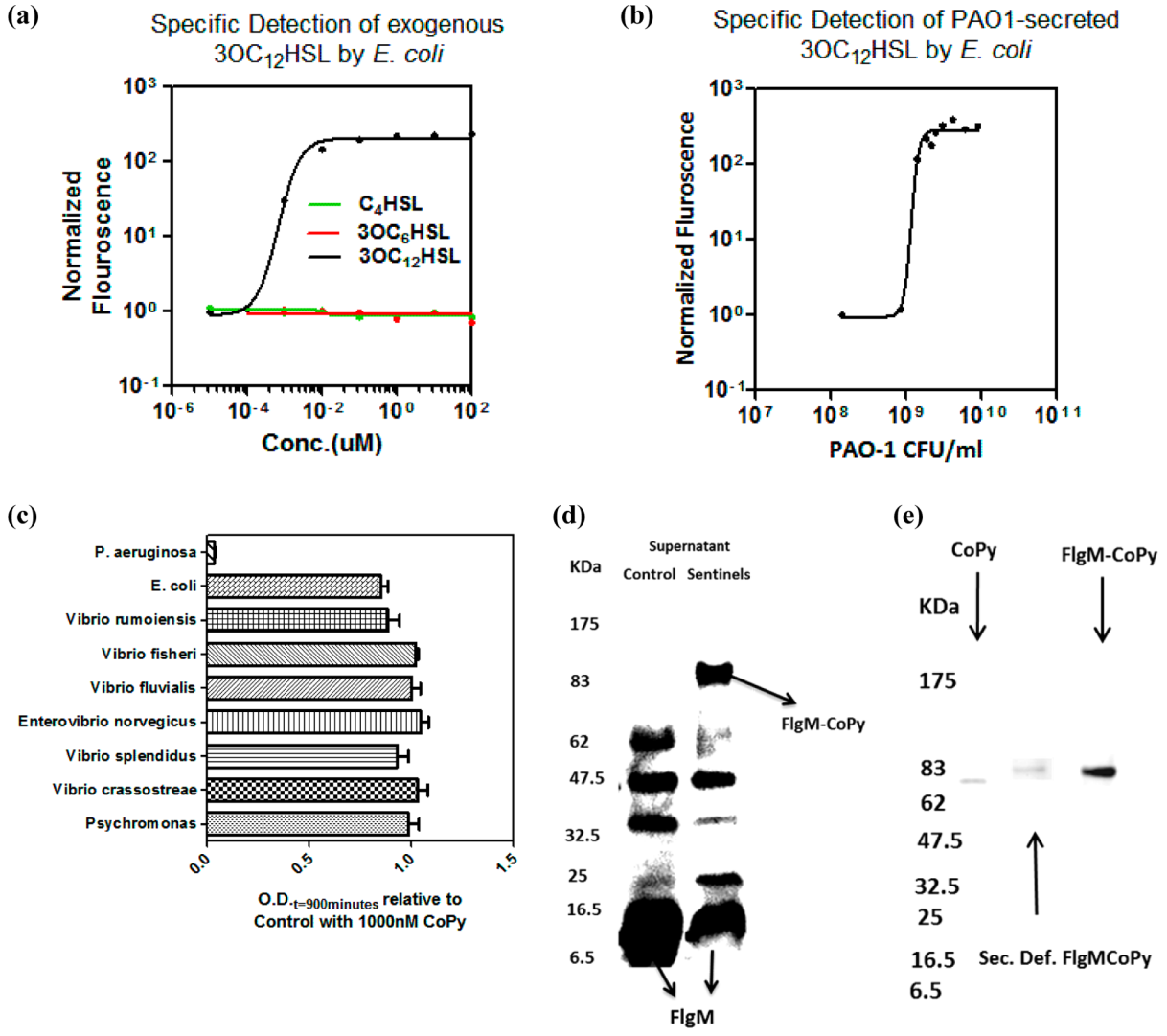

Figure 2. Testing the three modules. (a) Fluorescence of sentinels grown in various AHL concentrations. (b) Fluorescence of sentinels grown in PAO1 supernatant. (c) Comparison of the optical density at 900 min of growth relative to control for various strains exposed to 1000 nM CoPy. (d) Western blot of cells secreting His-FlgM-CoPy. From left: Lane 1 is protein ladder, lane 2 is control which is the concentrated supernatant of *E. coli.* MG1655, and lane 3 is the concentrated supernatant of *E. coli.* MG1655 transformed with plasmid pLHFC (pLas-His-FlgM-CoPy) + 10 μM $3OC_{12}HSL$. This blot was developed using anti-FlgM primary antibody. FlgMCoPy is present only in the concentrated supernatant from the sentinels. (e) Control to show that cells are exporting His-FlgM-CoPy because of FlgM secretion tag and not due to lysing. From left: Lane 1 is protein ladder, lane 2 is concentrated supernatant from *E. coli* cells expressing His-CoPy without FlgM secretion tag, lane 3 is concentrated supernatant from *E. coli* cells deficient in flagellar structures (*fla-*) expressing His-FlgM-CoPy, and lane 4 is concentrated supernatant from *E. coli* cells expressing His-FlgM-CoPy when induced with 10 μM $3OC_{12}HSL$. This blot was developed using anti-His primary antibody. Lane 2 shows basal level of His-CoPy, without any secretion tag, in the medium; lane 3 shows basal level of His-FlgM-CoPy in the medium when the producing cells are secretion deficient (*fla-*) because of the absence of flagellar structures; and lane 4 shows that by addition of FlgM secretion tag there is a marked increase in the amount of FlgM-CoPy, compared to His-CoPy, in the supernatant. If the export of His-FlgM-CoPy was due to cell lysis, then only basal levels of His-FlgM-CoPy similar to lane 3 would be present in the supernatant. This result demonstrates that the *E. coli* cells are able to secrete CoPy with the aid of FlgM in response to $3OC_{12}HSL$.

CoPy specificity was demonstrated by incubating 0.1 OD of nine different bacterial strains with 1 mM purified CoPy (Methods). For each growth assay, the change in optical density was measured over a 900 min time course and normalized to corresponding control cell growth in the absence of CoPy. As seen in Figure 2c, PAO1 growth is completely inhibited, whereas *E. coli* and the other tested bacterial strains display growth rates comparable to those of their controls (Figure 2c and Supplementary Figures S3, S6c, and S7).

Export of CoPy into the Extracellular Space of *E. coli*. In order to secrete CoPy using the flagellar system, FlgM was fused to the N-terminus of CoPy that was placed under the transcriptional control of Las promoter. This promoter is transcribed in the presence of LasR protein and $3OC_{12}HSL$, which is produced by PAO1. Western blotting was performed to validate secretion of CoPy using FlgM. The results demonstrate that His-FlgM-CoPy is present only in concentrated supernatant from sentinels expressing FlgM-CoPy under $3OC_{12}HSL$ induction (Figure 2d). Controls were performed to demonstrate that the presence of His-FlgM-CoPy in the extracellular medium is due to secretion and not cell lysis (Figure 2e).

In order to determine the efficiency of sentinel *E.* coli expression and secretion of FlgM-CoPy, cells were maximally

dx.doi.org/10.1021/sb4000417 | *ACS Synth. Biol.* 2013, 2, 715−723

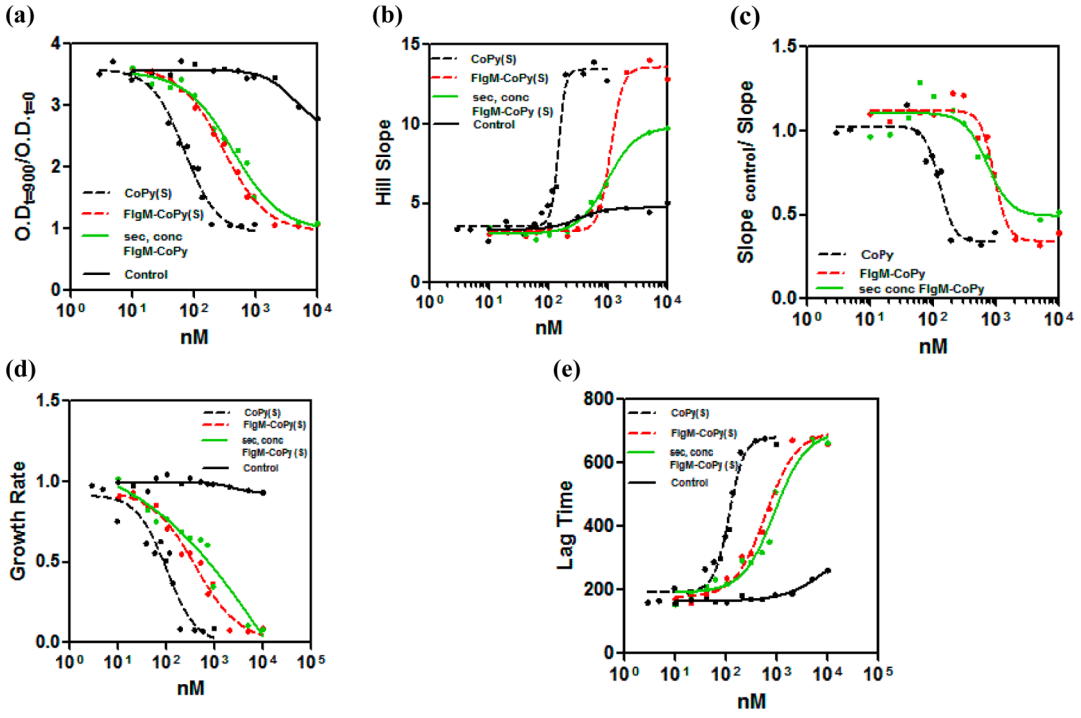

Figure 3. Analysis of growth curves of PAO1 under different concentrations of purified CoPy, nonsecreted FlgM-CoPy, and secreted FlgM-CoPy. (a) Half-maximal inhibitory concentration (IC_{50}) curve. (b) The Hill slope of various dosage−response curves calculated by nonlinear regression analysis. (c) Ratio of the Hill slope of control vs secreted, concentrated, and purified FlgM-CoPy. (d) Specific growth rate of PAO1 with different concentrations of secreted FlgM-CoPy. (e) Lag time of different growth curves of PAO1 for different concentrations of secreted FlgM-CoPy. All experiments were performed using 96 -well plates and a Tecan plate reader.

induced by 10 μM $3OC_{12}HSL$ and grown to an OD of 1. Separately, both total and secreted FlgM-CoPy were purified, collected, and quantified (as described in Methods). The total and secreted amounts of FlgM-CoPy were measured at 19.2 and 1.02 μg/1 mL, respectively. Hence, the approximate FlgM-CoPy secretion efficiency of *E. coli* sentinels is 5%.

Characterization of Purified CoPy and Nonsecreted and Secreted FlgM-CoPy. The effect of CoPy and FlgM-CoPy was analyzed by growing 0.1 OD of PAO1 in a 96-well plate with different amounts of purified protein (Supplementary Figure S3). Ratios of OD at 900 min to OD at 0 min were plotted for different dosage−response curves for purified control, CoPy, nonsecreted FlgM-CoPy, and secreted FlgM-CoPy (Figure 3a and Supplementary Figure S3). Half-maximal inhibitory concentration (IC_{50}) of CoPy and FlgM-CoPy were computed to be approximately 100 and 1000 nM respectively, indicating that IC_{50} of CoPy increased due to the addition of the FlgM secretion tag. IC_{50} is similar for nonsecreted and secreted FlgM-CoPy, indicating that the process of secretion itself has no observable effect on FlgM-CoPy's potency. Hill slope analysis for each dosage−response curve is also plotted for purified control, CoPy, and FlgM-CoPy (Figure 3b,c) and indicates a similar trend as IC_{50}.

Bacterial growth is visually divided into three phases: lag phase defined by a lag time (λ), exponential phase characterized by specific growth rate (μ_m), and stationary phase described by an asymptote (A; Supplementary Figure S4). In order to derive these parameters, the experimental data is described by a growth model and then μ_m, λ and A are estimated from the model.[23] With a sigmoidal dosage−response model, the values of λ, μ, and A are calculated by substituting the values of Top, Bottom, EC_{50}, and Hill slope estimated from the analysis (Supporting Information). The change in growth rate (μ) and lag time (λ) of PAO1 due to purified CoPy and FlgM-CoPy indicates that the toxin affects the growth and doubling time of PAO1 significantly (Figure 3d,e).

Sense and Destroy System. Once individual modules were validated, they were integrated to create the complete Sense and Destroy system. The number of sentinels needed to kill an individual PAO1 cell was computed in order to understand system dynamics (Methods). This was achieved by plotting growth curves of different numbers of PAO1 in concentrated sentinel supernatant (Figure 4a). Similar to Figure 3a, the ratio of PAO1 OD at 900 min versus 0 min for different numbers of sentinels per PAO1 cell was estimated (Figure 4b) to determine the half-maximal inhibitory ratio (IR_{50}) of 10^5 sentinels per PAO1 cell. This ratio was further validated by tracing Hill slope, lag time (λ), and growth rate (μ_m) for each curve (Figure 4c−f).

On the basis of these reults, we then setup a semisolid agar plate co-culture experiment by placing and observing a droplet of sentinels on a bed of PAO1 over time (Methods). In the corresponding negative control, *E. coli* cells detect PAO1 but do not produce FlgM-CoPy in response. Image analysis indicates that in the presence of sentinel *E. coli* cells (green fluorescence) capable of secreting FlgM-CoPy, at 7 h, the concentration of PAO1 (red fluorescence) is significantly lower (>30 fold; Supplementary Figure S8) and essentially undetectable, when compared to the negative controls (compare Figure 5a and b and Supplementary Figure S8).

Discussion. In this paper we develop a Pathogen Sense and Destroy system capable of detecting wild type PAO1 and responding by secreting a toxin that targets PAO1 specifically. We engineered a chimeric protein, CoPy, that inhibits PAO1

dx.doi.org/10.1021/sb4000417 | *ACS Synth. Biol.* 2013, 2, 715−723

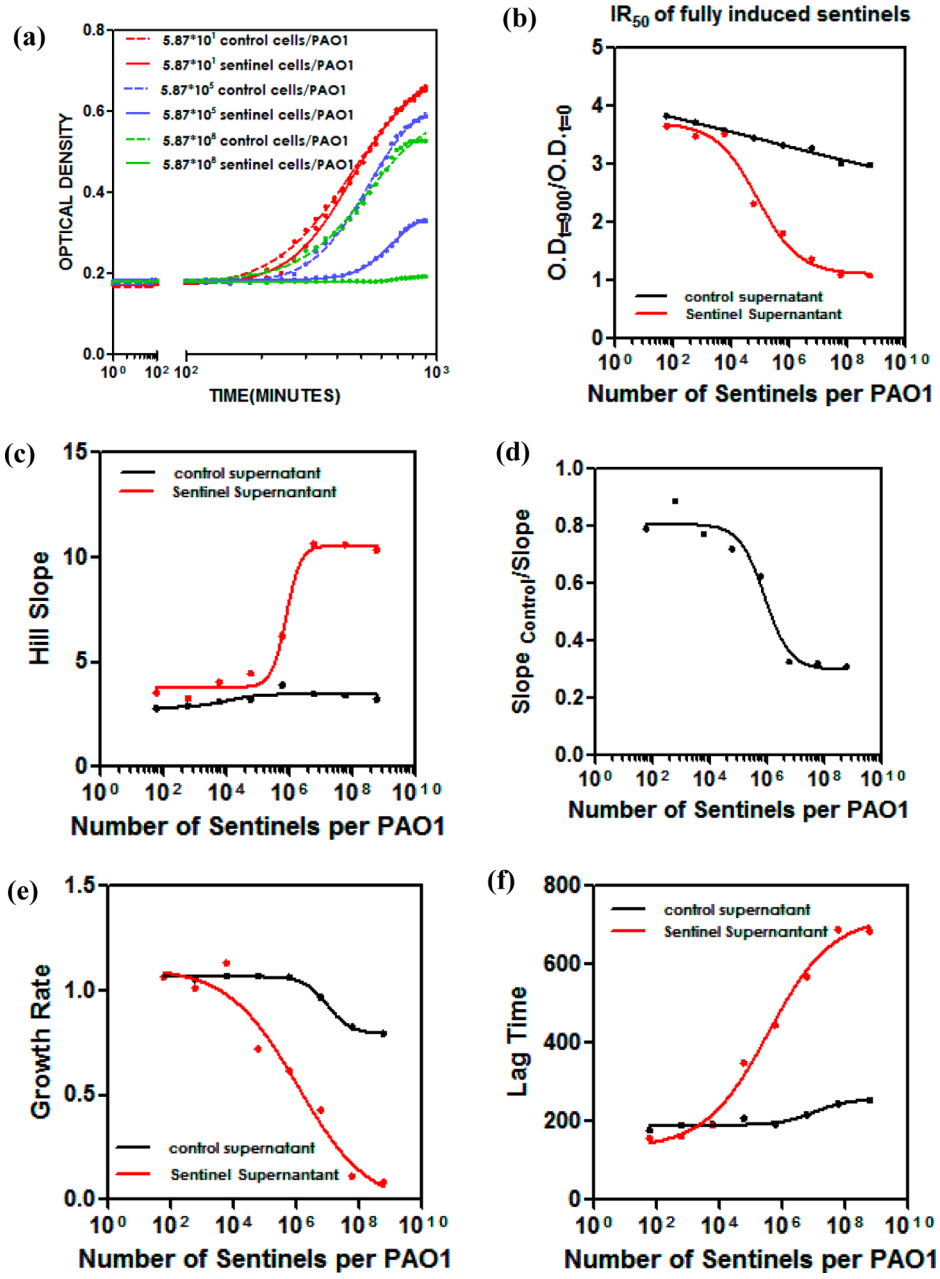

Figure 4. Analysis of PAO1 growth curves with concentrated supernatant from induced sentinels. (a) Three representative dosage−response curves with different ratios of sentinel/control cells vs PAO1. (b) Half-maximal inhibitory concentration (IC_{50}) curve for different ratios of sentinel/control cells vs PAO1. (c) The Hill slope of various dosage−response curves calculated by nonlinear regression analysis. (d) Ratio of the Hill slope of control vs sentinel supernatant. (e) Specific growth rate of PAO1 with different numbers of sentinels per PAO1. (f) Lag time of PAO1 growth curves with different numbers of sentinels per PAO1. All experiments were performed using 96-well plates and a Tecan plate reader.

growth specifically with an IC_{50} of 100 nM, while not affecting *E. coli* sentinels. FlgM was utilized as a secretion tag to transport CoPy into the extracellular medium without lysis of the producing cells and was capable of transporting ∼5% of total CoPy produced in the cytoplasm. This secretion efficiency is comparable to that achieved using other bacterial secretion strategies[24], whilst uniquely facilitating the secretion of large proteins such as FlgM-CoPy, with an observed mass of ∼84. kDa (Figure 2d). The IC_{50} of FlgM-CoPy is 1000 nM, which indicates that the addition of FlgM to CoPy increased the IC_{50} by a factor of 10. This was further verified by comparing Hill slope, growth rate, and lag time of PAO1 growth curves under different concentrations of CoPy and FlgM-CoPy. The Hill slope increased significantly with higher concentration of purified CoPy and FlgM-CoPy (Figure 3b). The Hill slope of the PAO1 growth curve with 2.88 nM CoPy is ∼3, and the Hill $slope_{control}$/Hill $slope_{CoPy}$ is ∼1. The Hill slope is ∼13 for PAO1 growth curve under 1000 nM of CoPy and the Hill $slope_{control}$/Hill $slope_{CoPy}$ is ∼0.23. For 1000 nM CoPy, optical density of PAO1 changed from OD_{min} of 0.18 to OD_{max} of 0.2 and no cell growth was observed (Figure 3d). Hence the minimum value of Hill $slope_{control}$/Hill $slope_{CoPy}$ attained in this experiment is 0.23.

Further quantitative analysis of the system properties revealed that in liquid culture settings ∼10^5 sentinel cells are needed to inhibit the growth of individual PAO1 cells (Figure

dx.doi.org/10.1021/sb4000417 | *ACS Synth. Biol.* 2013, 2, 715−723

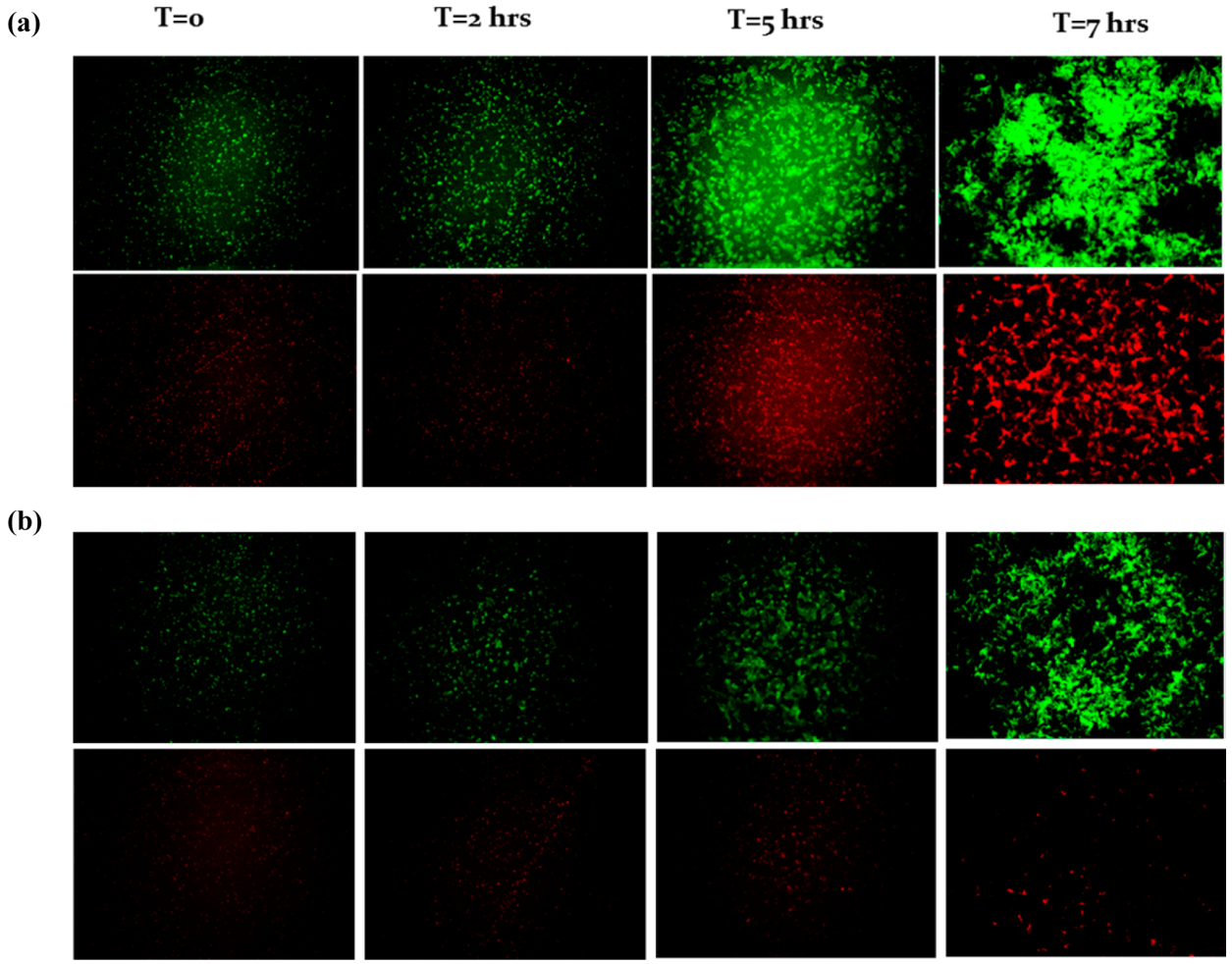

Figure 5. Microscopy images of sentinel droplet on a bed of PAO1. (a) Time-series microscopy images of a control *E. coli* droplet of cells on a PAO1 bed. (b) Time-series images of a FlgM-CoPy secreting *E. coli* sentinel droplet on a PAO1 bed of cells. PAO1 constitutively expresses red fluorescence, and *E. coli* sentinels and control cells constitutively express green fluorescence. PAO1 grows when co-incubated with the control cells; however, PAO1 growth is inhibited when co-incubated with the FlgM-CoPy secreting sentinels.

4b). Accordingly, our results further indicate that sentinel cells grown to an OD of 1 produce and secrete approximately 1μg/ml [20 nM] of CoPy, whereas PAO1 IC_{50} was measured at 1000 nM. Hence, in order to achieve significant (IC_{50}) levels of PAO1 growth inhibition, within normal bacterial growth concentrations, the system efficiency needs to increase by a factor of >50. System efficiency can possibly be improved in the future by increasing secretion efficiency and pathogen detection thresholds so that the sentinels begin to secrete large amounts of CoPy before PAO1 reaches high densities. The specificity and sensitivity of detection can likely be enhanced using directed evolution of the transcription factors.[25] Secretion efficiency can probably be improved by modifying the flagellar machinery involved in exporting native FlgM.[26-34] FlgM is 100 aa long, and its size is one of the factors affecting the secretion and growth inhibition efficacy. The minimum length of FlgM needed to secrete CoPy may be found by deletion studies. It is also possible that some FlgM-CoPy remains trapped in inclusion bodies because of excessive production of FlgM-CoPy and insufficient secretion. In a relevant study, the efficiency of FlgM secretion was improved in *fliS* and *fliT* mutants.[26]

Once we verified and evaluated the individual components of the Sense and Destroy system, the Sense, Secrete, and Destroy modules were integrated into a complete system, which was then used to assay its autonomous PAO1 growth inhibition dynamics in semisolid agar plate co-culture settings. The semisolid environment provides a rough approximation of bacterial micro-environments in the gastrointestinal tract.[35] In this semisolid environment, diffusion of FlgM-CoPy is reduced significantly in comparison to liquid medium and hence the local concentration of FlgM-CoPy per PAO1 cell is much higher than the average concentration of FlgM-CoPy for all PAO1 cells in a liquid medium. In this experimental setup, *E. coli* cells are also strongly induced because of the QS signals produced by the homogenously spread PAO1 in the plate. Therefore, significant growth inhibition of PAO1 (>30-fold; Supplementary Figure S8) by engineered *E. coli* sentinel cells is observed in the immediate vicinity of the droplet, where the FlgM-CoPy production and secretion requirements are met.

This work represents an advancement over a previously reported synthetic biology-driven antimicrobial strategy,[36] in which engineered *E. coli* sense *P. aeruginosa* by detecting $3OC_{12}HSL$ and commit suicide by lysing themselves to release pyocin S5. This pyocin-based killing strategy is effective only against the rare, pyocin S5-sensitive P. *aeruginosa ln7* strain and ineffective against the wild type and most other *Pseudomonas* strains. These strains are naturally resistant to pyocin S5, since

dx.doi.org/10.1021/sb4000417 | *ACS Synth. Biol.* 2013, 2, 715−723

they themselves naturally produce it. Furthermore, in our approach, *E. coli* self-lysis is avoided by creating sentinels that secrete FlgM-CoPy instead. The secreted toxin is engineered to target the pathogen specifically and does not affect the producing cells. Since our *E. coli* do not commit suicide in order to release the toxin, the approach can in principle support release of a different toxin if *P. aeruginosa* develops resistance to the original secreted toxin or if a different pathogen is detected at a later stage.

In future implementations, we may equip sentinel circuits with sophisticated logic for an adaptive response via sensing of the progression of PAO1 killing by the sentinels (e.g., by tracking $3OC_{12}HSL$ over time) and the deployment of different killing strategies as needed. Detection and destruction strategies could also be tailored to other target pathogens with sensing of particular quorum sensing molecules and toxins that are pathogen specific.

METHODS

Strains and Growth Conditions. *E. coli* K-12 MG1655 (F- lambda- *ilvG- rfb*-50 *rph*-1) and secretion deficient *E. coli* JE3513 (*fla*-) were obtained from the *E. coli* Genetic Stock Center at Yale University. *E. coli* DH5*a* (F- _80dlacZ_M15 _(lacZYA-argF)U169 recA1 endA1 hsdR17(rk-, mk+) phoA supE44 thi-1 gyrA96 relA1 E-) was used for plasmid construction and propagation. *E. coli* strain W3110 ColE3, ColI, StrR (cgsc no. 4963) was obtained from *E. coli* Genetic Stock Center at Yale University. Wild type *Pseudomonas aeruginosa* (PAO1) was a gift from Prof. Barbara H. Iglewski, University of Rochester Medical Center. Wild type *Pseudomonas aeruginosa* (PAO1) with constitutive *pilQ-mCherry* fluorescent fusion was a gift from Prof. Zemer Gitai, Princeton University. PAO1 is naturally resistant to 25 μg/mL of chloramphenicol. LB broth (Difco, Detroit, MI) with the appropriate antibiotic(s) was used as a growth medium in all experiments. For direct detection experiments, chloramphenicol [25 μg/mL] (Shelton Scientific, Shelton, CT) and ampicillin [100 μg/mL] (Sigma, St. Louis, MO) were used. For all growth experiments, cultures were incubated at 37 °C in a shaker at 280 rpm.

Plasmids. FlgM was PCR amplified from *E. coli* MG1655 genome. CoPy is a chimeric bacteriocin with receptor and translocase domain from pyocin S3 and nuclease and immunity domain from colicin E3. Colicin E3 was PCR amplified from *E. coli* strain W3110 ColE3, ColI, StrR (Genetic Stock Center at Yale University no. 4963). Similarly, pyocin S3 was PCR amplified from wild type PAO1. Pyocin S3 is a 767 amino acid protein with the first 637 amino acids encoding the translocation and receptor domains.[37] Similarly, the region of colicin E3 starting from *DraI* restriction enzyme site to the end of the genetic sequence represents the nuclease domain and immunity protein.[7] Chimeric bacteriocin CoPy was constructed by PCR SOEing the translocation and receptor domains from pyocin S3 to the nuclease and immunity domain of colicin E3. FlgM was PCR SOE'd to the N terminus of CoPy, resulting in chimeric protein FlgM-CoPy. A 6X amino acid His-tag was further PCR SOE'd to the N terminal of CoPy and FlgM-CoPy, which were subsequently cloned under $3OC_{12}HSL$ inducible pLas promoter using restriction enzymes resulting in plasmid pLas-His-CoPy (pLHC) and pLas-His-FlgM-CoPy (pLHFC). Plasmid pLas-His-FlgM (pLHF) was used as a control. Plasmids used in this study and their relevant properties are also listed in Supplementary Table S1.

Cell Density Measurements. Optical density (600 nm) readings were taken using a Tecan Safire[2] plate reader (Tecan-US, Durham, NC) at regular intervals over the course of the experiment. Total culture volume of purified CoPy or His-FlgM-CoPy in a well of a 96-well clear-bottom microtiter plate (Falcon, Oxnard, CA) was 200 μL. For long experiments, each well was incubated at 37 °C at 280 rpm and covered with 40 μL of mineral oil (ACROS Organics, USA) to prevent evaporation of the culture.

Detection of Exogenous and Endogenous $3OC_{12}HSL$ Produced by PAO1. Sentinels were grown to an OD of 0.5 and then induced and incubated with different concentrations of exogenous $3OC_{12}HSL$ for 3 h. The resulting fluorescence was measured with flow cytometry. PAO1 was grown to various different ODs, and supernatant was subsequently collected and filter sterilized. The supernatant contains endogenous signals produced by PAO1 for quorum sensing, but the cells are filter sterilized. After this, 0.5 OD of sentinels was incubated in the supernatant for 2 h, and their fluorescence was measured.

Protein Secretion, Purification, and Concentration Measurement. One liter of *E. coli* (DH5 alpha-pro) cells containing His-FlgM-CoPY were grown to an optical density of 0.05, and their expression was induced fully by 10 μM exogenous 3-oxo-dodecanoyl-homoserine lactone ($3OC_{12}HSL$ from CAYMAN Chemicals, item no. 10007895). Induced cultures were incubated at 37 °C and 280 rpm for 4 h. Subsequently the cells were pelleted by centrifugation at 6000 rpm for 20 min. Supernatant was collected and filter sterilized by a 0.22 μm NALGENE 500 mL low protein binding filter. This supernatant containing secreted His-FlgM-CoPy was concentrated by ultrafiltration using a 10-kDa molecular mass cutoff membrane in an AMICON stirred cell concentrator (Millipore, Billerica, MA, product no. 8400) until the volume was decreased to approx 70 mL. The retained medium was further concentrated using smaller centricon plus-70 (Millipore) centrifuge filtration devices with Ultracel PL-10 regenerated cellulose 10,000 MWCO (catalog no. UFC701008). Final volume of this retentate was 350 μL. Retentate was then His-Tag purified under native conditions using Ni-NTA (Ni^{2+}-nitrilotriacetate) Superflow (Qiagen) column, washed with 50 mM sodium phosphate buffer, 300 mM NaCl, and 10 mM imidazole (pH 7.4), and eluted with 50 mM $NaPO_4$, 300 mM NaCl, and 500 mM imidazole (pH 7.4). Purification using Co^{2+} ions from Clontech gave the same results. Protein concentration was determined via UV spectroscopy using a ThermoScientific, NanoDrop 2000c and the extinction coefficient (ε = 0.781) as calculated by the ProtPram tool on the ExPASy toolserver.[38]

Western Blot. Anti-FlgM antibody was kindly provided by Prof. Kelly Hughes from the University of Utah. Anti-His antibody was 6X His-Tag goat anti-rabbit IgG (1:10000) from Rockland Inc., USA. Anti-rabbit IgG, HRP-linked antibody no. 7074 (1:10000) from Cell Signaling was used as the secondary antibody, and 4−20% Mini-PROTEAN TGX precast polyacrylamide gels from Bio-Rad were used to run samples. Prestained broad range protein ladder from Cell Signaling (no. 7720) was used as the ladder. Mini-PROTEAN Tetra System from Bio-Rad was used for running Western blots. Trans-Blot SD Semi-Dry Transfer Cell from Bio-Rad was used to transfer the gel, which was run for 60 min at 120 V in Tris/glycine premixed electrophoresis buffer from Bio-Rad. For running Western blots, the gel was transferred to the Trans-Blot SD Semi-Dry Transfer Cell from Bio-Rad. The gel and membrane

sandwich was made according to the semidry transfer instructions. GE Healthcare Amersham ECL advance Western blotting detection kit was used according to manufacturer's instructions for developing the membrane, and a Bio-Rad imager (Molecular Imager Gel Doc XR+ System with Image Lab Software from Bio-Rad, Hercules, CA, USA) was used for imaging the gel.

Experimental Setup To Calculate the Number of Sentinels Needed To Kill One PAO1. A 100 mL portion of PAO1 was grown to an OD of 1. Then, PAO1 was removed from the culture by passing it through a sterile 0.22 μm filter and collecting the supernatant. This 100 mL of filter-sterilized supernatant has the quorum sensing molecules produced by PAO1. At an OD of 1, PAO1 were observed experimentally to maximally induce sentinel expression (Figure 2b). Subsequently, sentinels were grown in this supernatant in order to characterize their response to these QS molecules. Since the sentinels secrete FlgM-CoPy in response to PAO1 QS signal, the resulting cell culture should contain secreted FlgM-CoPy from the sentinels. The sentinels were then removed from the culture, and the supernatant was concentrated (400X) using a 10 KDa filter membrane (Centricon Plus-70 centrifugal units with 10,000 NMWL Ultracel PL-10 membrane from Millipore). Final volume of the retentate was 250 μL, containing the FlgM-CoPy (84 KDa) secreted by the sentinels. Presence of FlgM-CoPy in the supernatant was verified by Western blot. Different initial concentrations of PAO1 were grown in 50 μL of the concentrated supernatant per well in a 96-well plate; 50 μL of the concentrated supernatant is equivalent to the supernatant from 20 mL of maximally induced sentinels with an OD 1.26 or 17.6 $\times$ 10^9 sentinels (Supplementary Figure S4).

Microscopy Cell Imaging. The solid phase co-culture experiment was performed at 37 °C. Briefly, 100 μL of PAO1, expressing constitutive red fluorescent protein, at OD 0.001 was evenly spread on an 85 mm wide Petri dish filled with 40 mL of LB agar (Supplementary Figure S5). The 10 μL of the sentinels/control cells (*E. coli*, MG1655 + pLHFC) at an OD of 1 were pipetted on the agar surface, forming a 4 mm wide circle, containing approximately 3 $\times$ 10^7 sentinel and 150 PAO1 cells. The plate was then incubated at 37 °C, and images were taken every hour using a Zeiss (Thornwood, NY) Axiovert 200 M microscope equipped with an AxioCam MR CCD camera. The images were taken with 10X objective and a GFP filter (470/40 excitation, 525/50 emission) and DsRed Express filter (565/30 excitation and 620/60 emission). ImageJ software[39] was used for image fluorescence intensity quantification, which was represented as mean field fluorescence intensity (Supplementary Figure S8).

■ ASSOCIATED CONTENT

Supporting Information

Equations, supplementary figures (S1–S8), and a table of DNA constructs used in the work. This material is available free of charge via the Internet at http://pubs.acs.org.

■ AUTHOR INFORMATION

Corresponding Author

*Tel: 617-253-8966. E-mail: rweiss@mit.edu.

Author Contributions

S.G. conceptualized the project, designed and preformed the experiments, and collected and interpreted the data. E.E.B. contributed to the revision, data analysis. and interpretation. R.W. conceptualized the project, designed experiments. and interpreted the data. All authors contributed to writing the manuscript.

Notes

The authors declare no competing financial interest.

■ ACKNOWLEDGMENTS

This work was supported by the Office of Naval Research, Award No. 13PR02978-00 A00001 and by the Bill and Melinda Gates Foundation, Grant No. OPP1024433.

■ REFERENCES

(1) Finch, R. G. (2004) Antibiotic resistance: a view from the prescriber. *Nat. Rev. Microbiol. 2*, 989–994.

(2) Na, X., and Kelly, C. (2011) Probiotics in clostridium difficile Infection. *J. Clin. Gastroenterol. 45* (Suppl), S154–158.

(3) Gough, E., Shaikh, H., and Manges, A. R. (2011) Systematic review of intestinal microbiota transplantation (fecal bacteriotherapy) for recurrent Clostridium difficile infection. *Clin. Infect. Dis. 53*, 994–1002.

(4) Cotter, P. D., Hill, C., and Ross, R. P. (2005) Bacteriocins: developing innate immunity for food. *Nat. Rev. Microbiol. 3*, 777–788.

(5) Parret, A. H., and De Mot, R. (2002) Bacteria killing their own kind: novel bacteriocins of Pseudomonas and other gamma-proteobacteria. *Trends Microbio.l 10*, 107–112.

(6) Cascales, E., et al. (2007) Colicin biology. *Microbiol. Mol. Biol. Rev. 71*, 158–229.

(7) Kageyama, M., Kobayashi, M., Sano, Y., and Masaki, H. (1996) Construction and characterization of pyocin-colicin chimeric proteins. *J. Bacteriol. 178*, 103–110.

(8) Mergulhao, F. J., Summers, D. K., and Monteiro, G. A. (2005) Recombinant protein secretion in Escherichia coli. *Biotechnol. Adv. 23*, 177–202.

(9) Saier, M. H., Jr. (2006) Protein secretion and membrane insertion systems in gram-negative bacteria. *J. Membr. Biol. 214*, 75–90.

(10) Sandkvist, M., and Bagdasarian, M. (1996) Secretion of recombinant proteins by Gram-negative bacteria. *Curr. Opin. Biotechnol. 7*, 505–511.

(11) Wickner, W., and Schekman, R. (2005) Protein translocation across biological membranes. *Science 310*, 1452–1456.

(12) Sorensen, H. P., and Mortensen, K. K. (2005) Advanced genetic strategies for recombinant protein expression in Escherichia coli. *J. Biotechnol. 115*, 113–128.

(13) Filloux, A., Hachani, A., and Bleves, S. (2008) The bacterial type VI secretion machine: yet another player for protein transport across membranes. *Microbiology 154*, 1570–1583.

(14) Georgiou, G., and Segatori, L. (2005) Preparative expression of secreted proteins in bacteria: status report and future prospects. *Curr. Opin. Biotechnol. 16*, 538–545.

(15) San Miguel, M., Marrington, R., Rodger, P. M., Rodger, A., and Robinson, C. (2003) An Escherichia coli twin-arginine signal peptide switches between helical and unstructured conformations depending on the hydrophobicity of the environment. *Eur. J. Biochem. 270*, 3345–3352.

(16) Bernard, C. S., Brunet, Y. R., Gueguen, E., and Cascales, E. (2010) Nooks and crannies in type VI secretion regulation. *J. Bacteriol. 192*, 3850–3860.

(17) Bingle, L. E., Bailey, C. M., and Pallen, M. J. (2008) Type VI secretion: a beginner's guide. *Curr. Opin. Microbiol. 11*, 3–8.

(18) Feltcher, M. E., Sullivan, J. T., and Braunstein, M. (2010) Protein export systems of Mycobacterium tuberculosis: novel targets for drug development? *Future Microbiol. 5*, 1581–1597.

(19) Delepelaire, P. (2004) Type I secretion in gram-negative bacteria. *Biochim. Biophys. Acta 1694*, 149–161.

(20) Aldridge, P., Gnerer, J., Karlinsey, J. E., and Hughes, K. T. (2006) Transcriptional and translational control of the Salmonella fliC gene. *J. Bacteriol. 188*, 4487−4496.
(21) Chilcott, G. S., and Hughes, K. T. (2000) Coupling of flagellar gene expression to flagellar assembly in Salmonella enterica serovar typhimurium and Escherichia coli. *Microbiol. Mol. Biol. Rev. 64*, 694−708.
(22) Karlinsey, J. E., et al. (2000) Completion of the hook-basal body complex of the Salmonella typhimurium flagellum is coupled to FlgM secretion and fliC transcription. *Mol. Microbiol. 37*, 1220−1231.
(23) Zwietering, M. H., Jongenburger, I., Rombouts, F. M., and van 't Riet, K. (1990) Modeling of the bacterial growth curve. *Appl. Environ. Microbiol. 56*, 1875−1881.
(24) Gupta, P., and Lee, K. H. (2008) Silent mutations result in HlyA hypersecretion by reducing intracellular HlyA protein aggregates. *Biotechnol. Bioeng. 101*, 967−974.
(25) Collins, C. H., Arnold, F. H., and Leadbetter, J. R. (2005) Directed evolution of Vibrio fischeri LuxR for increased sensitivity to a broad spectrum of acyl-homoserine lactones. *Mol. Microbiol. 55*, 712−723.
(26) Aldridge, P. D., et al. (2006) The flagellar-specific transcription factor, sigma28, is the Type III secretion chaperone for the flagellar-specific anti-sigma28 factor FlgM. *Genes Dev. 20*, 2315−2326.
(27) Chadsey, M. S., and Hughes, K. T. (2001) A multipartite interaction between Salmonella transcription factor sigma28 and its anti-sigma factor FlgM: implications for sigma28 holoenzyme destabilization through stepwise binding. *J. Mol. Biol. 306*, 915−929.
(28) Chevance, F. F., Karlinsey, J. E., Wozniak, C. E., and Hughes, K. T. (2006) A little gene with big effects: a serT mutant is defective in flgM gene translation. *J. Bacteriol. 188*, 297−304.
(29) Daughdrill, G. W., Hanely, L. J., and Dahlquist, F. W. (1998) The C-terminal half of the anti-sigma factor FlgM contains a dynamic equilibrium solution structure favoring helical conformations. *Biochemistry 37*, 1076−1082.
(30) Frisk, A., Jyot, J., Arora, S. K., and Ramphal, R. (2002) Identification and functional characterization of flgM, a gene encoding the anti-sigma 28 factor in Pseudomonas aeruginosa. *J. Bacteriol. 184*, 1514−1521.
(31) Hughes, K. T., Gillen, K. L., Semon, M. J., and Karlinsey, J. E. (1993) Sensing structural intermediates in bacterial flagellar assembly by export of a negative regulator. *Science 262*, 1277−1280.
(32) Schmitt, C. K., Darnell, S. C., and O'Brien, A. D. (1996) The attenuated phenotype of a Salmonella typhimurium flgM mutant is related to expression of FliC flagellin. *J. Bacteriol. 178*, 2911−2915.
(33) Schmitt, C. K., Darnell, S. C., Tesh, V. L., Stocker, B. A., and O'Brien, A. D. (1994) Mutation of flgM attenuates virulence of Salmonella typhimurium, and mutation of fliA represses the attenuated phenotype. *J. Bacteriol. 176*, 368−377.
(34) Yokoseki, T., Iino, T., and Kutsukake, K. (1996) Negative regulation by fliD, fliS, and fliT of the export of the flagellum-specific anti-sigma factor, FlgM, in Salmonella typhimurium. *J. Bacteriol. 178*, 899−901.
(35) Kim, J., Hegde, M., and Jayaraman, A. (2010) Co-culture of epithelial cells and bacteria for investigating host-pathogen interactions. *Lab Chip 10*, 43−50.
(36) Saeidi, N., et al. (2011) Engineering microbes to sense and eradicate Pseudomonas aeruginosa, a human pathogen. *Mol. Syst. Biol. 7*, 521.
(37) Michel-Briand, Y., and Baysse, C. (2002) The pyocins of Pseudomonas aeruginosa. *Biochimie 84*, 499−510.
(38) Gasteiger, E., et al. (2003) ExPASy: The proteomics server for in-depth protein knowledge and analysis. *Nucleic Acids Res. 31*, 3784−3788.
(39) Schneider, C. A., Rasband, W. S., and Eliceiri, K. W. (2012) NIH Image to ImageJ: 25 years of image analysis. *Nat. Methods 9*, 671−675.